Journal of Saudi Chemical Society (2015) **19**, 595–601

King Saud University

Journal of Saudi Chemical Society

www.ksu.edu.sa
www.sciencedirect.com

ORIGINAL ARTICLE

Photoelectric conversion performances of Mn doped TiO_2 under >420 nm visible light irradiation

Lijie Wang [a], Xi Zhang [a], Peng Zhang [a], Zetan Cao [a], Junhua Hu [a,b,*]

[a] *School of Materials Science and Engineering, Zhengzhou University, Zhengzhou 450002, Henan Province, PR China*
[b] *International Joint Research Laboratory for Low-carbon & Environmental Materials of Henan Province, Zhengzhou 450002, Henan Province, PR China*

Received 14 February 2015; revised 10 April 2015; accepted 2 May 2015
Available online 14 May 2015

KEYWORDS

Mn doped TiO_2;
X-ray photoelectron spectroscopy;
Visible light

Abstract Mn doped TiO_2 was synthesized by hydrothermal treatment of titanium boride and manganese chloride. The doped nano powders were fabricated by adding ammonium water into the mother solution which was obtained hydrothermally. The calcination of precursory powders took place at the temperature of 400–600 °C which resulted in the formation of anatase with a small amount of rutile phase. The shift of valence band maximum (VBM) toward the lower binding energies was observed by measuring the position of VBM with reference to the Fermi level, which contributed to the significant red-shift of absorption edges. X-ray photoelectron spectroscopy (XPS) measurement shows that manganese exists in both 4+ and 3+ valance states, which may have a temperate replacing of Ti^{4+} because of the charge compensation compared with 2+ and 3+ valence states. The property of photoelectric conversion was detected by evaluating the photocurrent under visible light (>420 nm), and the fluorescence spectra also proved that 6%-Mn doped TiO_2 (DM6) shows a better photoelectric conversion performance.

1. Introduction

Global environmental and energy crisis demand for high performance and low cost semiconductors, which can transform solar energy to electric energy. So many researchers have devoted efforts to the physical and chemical researches of semiconducting TiO_2. The fundamental limitation due to the wide band gap of TiO_2 (3.2 eV for anatase), makes it rather ineffective for visible light which accounts for more than 50% in the whole solar spectrum [1,2]. To break through the UV limitation of TiO_2 in anatase and rutile phases, extensive experimental and theoretical work has been conducted toward doping TiO_2 with both transition metal and nonmetal dopants to utilize the whole spectrum of solar light, which will promote the potential for a wide range of prospective applications such as pure inorganic oxide solar cell, photocatalyst for degradation organic pollutants, feasible water splitting and air purification [3–8]. And also noble

* Corresponding author at: School of Materials Science and Engineering, Zhengzhou University, Zhengzhou 450002, Henan Province, PR China. Tel.: +86 371 67739533.
E-mail address: Hujh@zzu.edu.cn (J. Hu).
Peer review under responsibility of King Saud University.

Production and hosting by Elsevier

http://dx.doi.org/10.1016/j.jscs.2015.05.001

metal (Au, Ag, Pt etc.) deposition gives evidences about electron relay effect to enhanced visible light activity [9–15], besides, binary metal oxide photocatalytic degradation researched by A. Stephen and co-workers give another direction to reduce the influence of the wide band gap [16–18]. The significant red shift effect of band edges of doped TiO_2 can be contributed to narrowing the bandgap, introduction of an intermediate band (IB), and the formation of color center or localized states in the band gap. Latest news show that the nature of visible light response coming from photoinduced electron traps has been explored by excellent scientific research workers [19].

Various molecular design theories are trying to chart a road map for effective doping formulation. The consistent results of the experiment and calculation have helped researchers to clarify the origin of visible light performance by doping. In our previous work, the doping effect and the origin of visible light absorption of several 3d transition metals, including V, Ga, Cr, Fe, Mn, Co, Ni, Cu, and Zn doping in TiO_2 investigated, using a molecular design approach within the framework of the density functional theory (DFT), with Hubbard U correction (DFT + U) for necessary refinement in the modeling [20–22]. The results of modeling indicate that Mn substitution of the Ti lattice sites has the biggest potential among 3d transition metals, for the reduction of energy gap and the introduction of effective intermediate bands (IBs) to allow multi-band optical absorption.

Mn-doped TiO_2 was recently implemented in the case of photocatalytic and solar-driven water splitting, which mostly uses $TiOSO_4{\cdot}xH_2O$, $Ti(OCH(CH_3)_2)_4$ [23] or tetrabutyl titanate as Ti resource. However, the doping in neutralizing process of the mother solution gives rise to the equilibrium doping. Ruby Chauhan [24] reported his Mn doped TiO_2 for structural and photocatalytic studies while there did not seem much bandgap narrowing as to their Mn^{2+} doping. Our team reported Mn-doped TiO_2 thin film by magnetron sputtering [38] and Mn^{4+}/Mn^{3+} doped photocatalytic [25] before. By comparing the doping methods, maybe the formation of titanium manganate or titanate including manganese ion after neutralizing (Fig. 1a) reaction gives a new way for preparing the precursor of doped TiO_2, which exhibits a better doping efficiency after the heat treatment of that precursor. In this work, a Mn doped TiO_2 was synthesized by hydrothermal treatment of titanium boride to get the mother solution. TiO_2 was precipitated by adding ammonium water into the hydrothermally obtained transparent solution, what is interesting is that the temperature of crystal and phase transition was greatly influenced by the different doping levels. It has been found that the Mn-doped TiO_2 nano particles exhibit much higher photoelectrochemical performances than pure TiO_2 under visible light irradiation. All the structure characterizations were made to speculate the indirect relationship between the solar energy utilization and photoelectric conversion, Mn^{4+} may play the key role for its absorption of visible light and low charge difference of metal ion. Also the fluorescence spectra give the evidence of hydroxyl radical (·OH) production of Mn-doped TiO_2 only under >420 nm visible light irradiation, combined with the photocurrent.

2. Experiment

Hydrochloric acid (36.5–38% by weight ratio) was mixed with deionized water by the volume ratio 1:3 in a Teflon lined stainless steel autoclave. Titanium boride powder (Aladdin, 4–8 μm), which does not react with both HF and HCl in ambient conditions, was added into the autoclave together with $MnCl_2$ (Alfa, America) powder. The content of Mn was controlled by atomic percentage $MnCl_2/TiB_2$ in a ratio 0∼10%. For the convenience of description, the samples are referred according to the Mn content, therefore, the DMx refers to powders with nominal Mn content of x%. The autoclave was kept at 180 °C for 30 h. After it was cooled to room temperature, a violet and transparent solution was obtained. Then, ammonia water (25%, Sinopharm Chemical Regent) was added into the above aqueous solution, which led to the formation of Mn-doped TiO_2 precursor. The precursor was collected by centrifugation and fully washed with deionized water to remove any dissolvable impurity. After drying at 80 °C in air, the precursor was annealed to get Mn doped crystalline TiO_2.

2.1. Characterization

The diffused reflectance spectra of the catalysts were recorded on a UV–Vis spectrophotometer (Shimadzu, model UV3600) in the range of 200 to 800 nm and standard $BaSO_4$ powder was used as a reference. The morphology of the TiO_2 powder was observed by HR-TEM (FEI JEM-2100). X-ray diffraction (XRD) measurements were carried out using Rigaku Ultima IV with CuKa radiation (wavelength = 0.15406 nm) from 20° to 80° at a scanning speed of 2°/min. XPS of the catalysts was performed on an ESCALAB 250 spectrometer (Thermo Scientific Ltd. England) with AlKa (1486.6 eV) radiation as the source. Raman spectra were collected by using Lab RAM HR 800 evolution. Photocurrent under visible light irradiation was recorded with a potentiostat (AMETEK, PARSTAT 4000) in a sandwich-type configuration using Pt slice as the counter electrode, a saturated calomel electrode (SCE) as the reference, and 0.1 M Na_2SO_4 solution as electrolyte. The Mn doped TiO_2 nano powder was used as photoelectrode (coating on FTO) in the 3-electrode electrochemical cell. A 300 W xenon arc lamp equipped with an ultraviolet cutoff filter ($\lambda > 420$ nm, Shanghai Lansheng Sci-tech Co. Ltd., China). Fluorescence measurements (Tianjin Gangdong F-280) were used to detect the number of hydroxyl radicals induced by terephthalic acid, and the excitation wavelength chosen as 320 nm.

3. Results and discussion

TiB_2 is the most stable of several titanium-boron compounds and does not react with both HF and HCl in ambient condition. It was used as a raw material to fabricate TiO_2 powder by the hydrothermal process. Therein, interstitial $B^{\sigma+}$ ($\sigma \leqslant 3$) ion can weaken the Ti–O bond and make the lattice doping more feasible [2]. In this work, the hydrothermally obtained solution shows a light violet color (the left one in the inset of Fig. 1a) after reaction. PH value of the solution was 5.0. After neutralization by ammonium water, the flocculent precipitate was formed and the solution became colorless (the right one in the inset of Fig. 1a). To analyze the ions involved in the precipitin reaction, the UV–Vis spectra of solution before and after neutralization were recorded. Peaks in Fig. 1a were compared with the established curves of standard

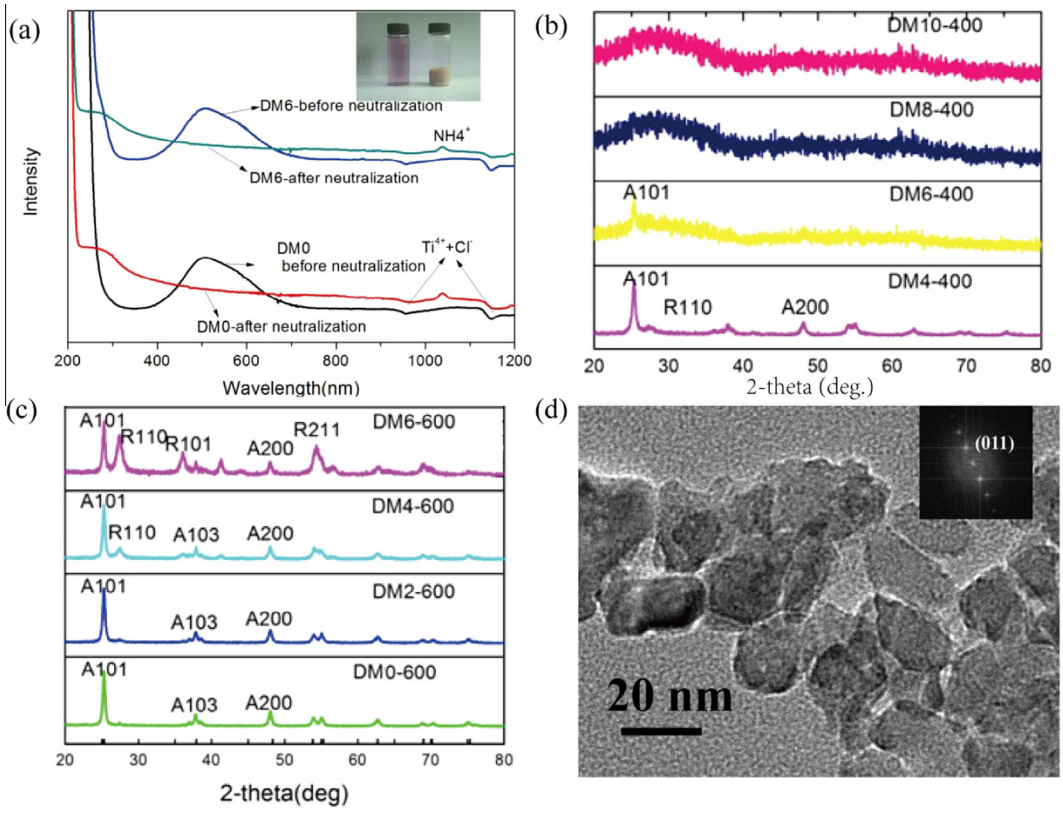

Figure 1 (a) UV–Vis absorption spectra of the solution before and after neutralization; (b) XRD patterns of samples calcined at 400 °C; (c) XRD patterns of samples calcined at 600 °C; (d) TEM image of DM6.

solution as NH^{4+}, Ti^{4+} (in HCl) etc. Before the addition of ammonium water, the solution contained Ti^{4+}, Cl^{-} and H^{+}, while the NH^{4+} peak was detected after neutralization. The flocculent precipitate was examined by XRD and was proved in the amorphous state. The crystallization of anatase (Fig. 1b) occurred when calcined at 400 °C. A small amount of the rutile phase in DM4 was confirmed by the XRD pattern as shown in the bottom panel in Fig. 1b. With the increase of Mn content, the formation of the anatase phase needs higher temperature, but obviously the phase-transition temperature from anatase to rutile decreased. For DM8 and DM10, the anatase crystallization occurred at the temperature of near 600 °C. If Mn content is higher than 8 at.%, the rutile phase became the dominant phase.

Fig. 1d shows that typical TEM morphology image of the Mn doped sample (DM6). Samples consist of well dispersed nano particles with a uniform size of 20 nm. The selected-area electron diffraction of DM6 after sintering at 600 °C was displayed in Fig. 2a, which was proofed as an anatase phase. Sintering of DM0 and DM2 at 600 °C has resulted in

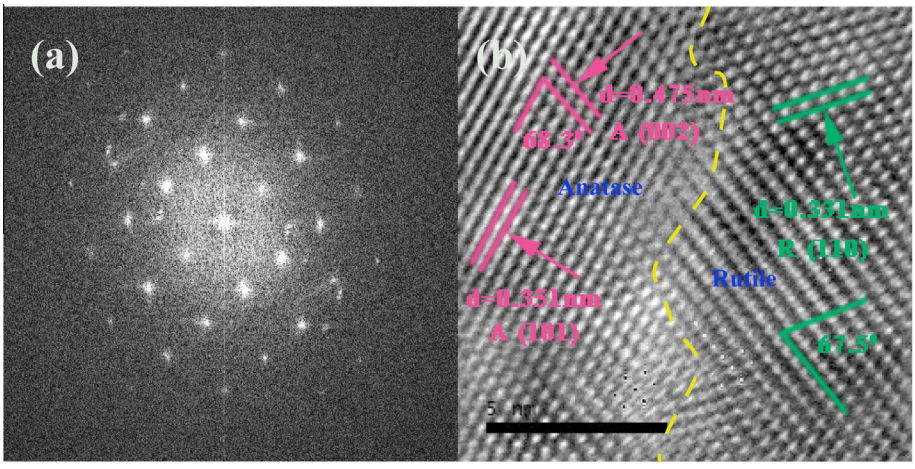

Figure 2 (a) Selected-area electron diffraction of DM6 (anatase); (b) HRTEM of DM6.

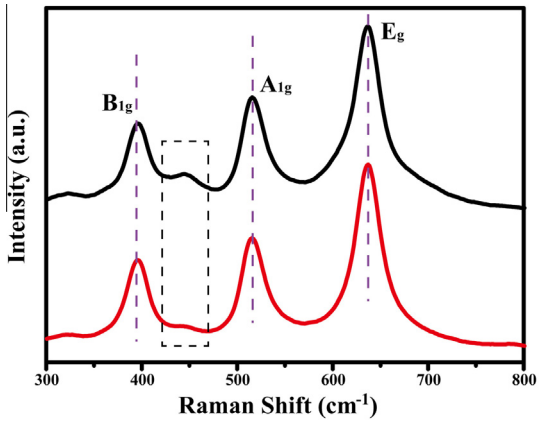

Figure 3 Raman spectra of the pure TiO_2 and DM4 sample (red line: pure TiO_2; black line: DM4).

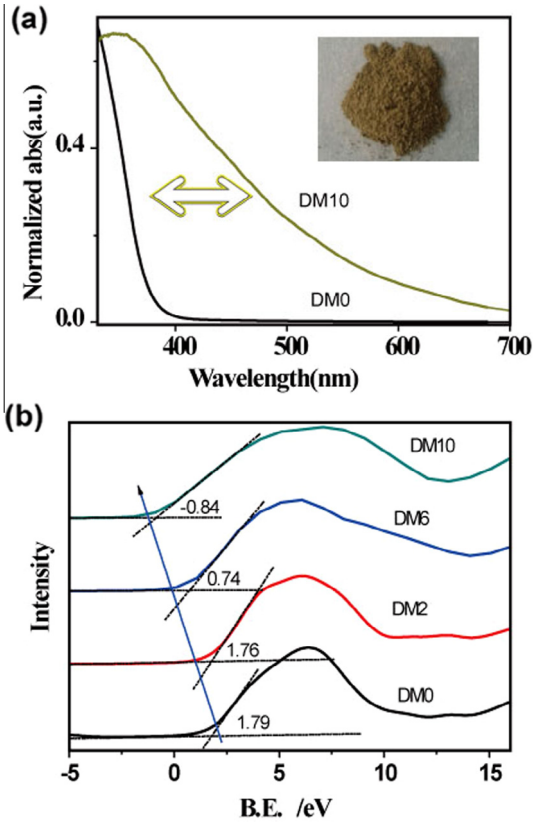

Figure 4 (a) UV–Vis absorption spectra of pristine TiO_2 and DM 10. (b) VBXPS spectra of doped TiO_2, with an arrow-headed line guiding the evident elevation in the VBM due to Mn doping.

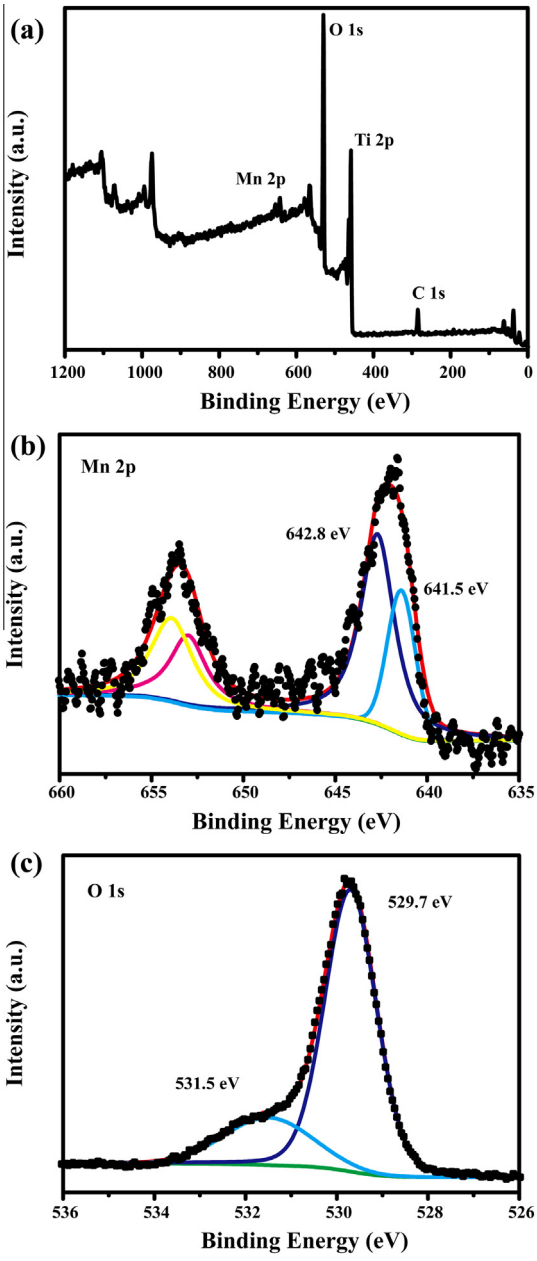

Figure 5 XPS spectrogram of Mn-doped (4%) TiO_2; (a) survey spectrum; (b) spectra focused on the Mn 2p; (c)spectra focused on the O 1s.

the crystallization of a single anatase phase. In Fig. 2b, it was found that the rutile phase began to grow around the anatase when the DM6 was calcined at 600 °C, which agrees with the XRD result. The yellow dotted line indicates the phase boundary of the two phases. It is observed that (0 0 2) facet serves as a habit face for the growth of rutile (1 1 0) [26]. The distance mismatch between them was just 0.02 nm.

Raman spectroscopy was used to detect the possible influence of manganese doped on the geometric structure of TiO_2. Anatase shows six active modes, namely, Eg(1), Eg(2), Eg(3), B1g(1), B1g(2) and A1g, with frequencies at 144, 197, 639, 399, 519, and 513 cm^{-1},respectively.[27] An additional active mode ranging from 430 to 480 cm^{-1} (Fig. 3) is observed in the doped TiO_2, which is not attributed to any TiO_2 phase. So a possible explanation for this situation is that substitutional manganese doped in the lattice of TiO_2, changed the typical anatase TiO_2 Raman selection rules by lowering the geometric symmetries of TiO_2 [1]. In our case, Ti–O–Mn may be responsible for this mode.

With the increase of Mn content from 0% to 10%, the color changed from white to dark brown. The absorption edges of Mn doped samples can be shifted continuously to 700 nm when the Mn content reached to 10 at.%. Fig. 4 a shows the UV–Vis

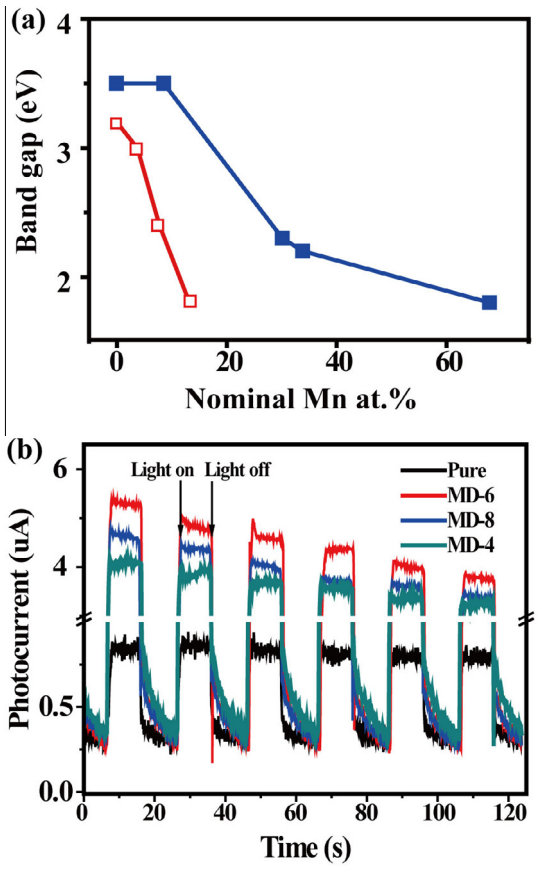

Figure 6 (a) Comparison of the doping effect of magnetron sputtering (filled square) and current work (open square). (b) Photocurrent driven by visible light for DM0–DM8.

comparison diagram of pure TiO_2 and DM10. High-resolution valence band XPS (VBXPS) was employed to probe the origin of the red-shift in the optical absorption edges of Mn-doped TiO_2, which provides spectra proportional to the occupied density of state (DOS) and has thus been used to investigate the electronic structures of the Mn-doped TiO_2 samples [28–30]. As seen from Fig. 4b, the valence band maximum shifted toward the lower binding energies and the overall valence band width increases with increasing Mn content. As the Mn doping level reached 10%, the valence band edge was shifted from 1.79 to −0.84 eV. This indicates that Mn doping induced considerable energetic elevation of the VBM, which could contribute to narrowing the overall energy gap in the doped materials. The TiO_2 VB is composed mainly of the occupied O 2p states with some minor contributions from metal (Ti) 3d states. The shape of VB spectra can be related to the chemical states of oxygen in TiO_2 [31,32]. The presence of oxygen vacancy will flatten the top of the valence band (VB) and change the peaks into a plateau. In such a case, it can be concluded that the sample of Mn doped TiO_2 is with low content of oxygen vacancy. According to some DFT calculations using different exchange–correlation (XC) functions [33], the appearances of oxygen vacancies in TiO_2 will induce a donor level next to the CBM and mid-gap (deep level) defect states, without any evident effect on reducing the overall energy gap.

The qualitative results of the XPS experiments are displayed in Fig. 5. Survey spectra were taken (Fig. 5a) and the presence of manganese and oxygen was evidenced. The presence of Mn 2p1/2 (642.8 eV) peaks associated with Mn^{4+} and 641.5 eV is attributed to Mn^{3+} in Fig. 5b, respectively [34]. Fig. 5c focuses on the O 1s binding energy at 529.7 eV (lattice TiO_2 oxygen atoms) with a shoulder centered at 531.5 eV. This latter feature is due to the presence of OH surface groups and possibly adsorbed water [35]. As we mentioned above, the samples have a quite low content of oxygen vacancy, which corresponds to the higher oxidation state of manganese [36,37].

Fig. 6a displays the comparison of doping effect of magnetron sputtering (as filled square) and current work (as open square). It is clearly demonstrated that almost the same band-gap narrowing effect can be achieved while the Mn content is just 1/5 of that in Ref. [38]. It had been confirmed that the magnetron sputtered TiO_2 contained a high density of oxygen vacancy due to the thermodynamically nonequilibrium growth condition.

According to the shift of VBM toward the lower binding energies, the absorption peak edges red-shifted continuously. However, the actual measurements of visible light driven photoelectric conversion performances did not really confirm this trend as shown in Fig. 6b. 6%-Mn doped TiO_2 shows a superior photoelectric conversion performance which largely improved compared with pure TiO_2. It is believed that the

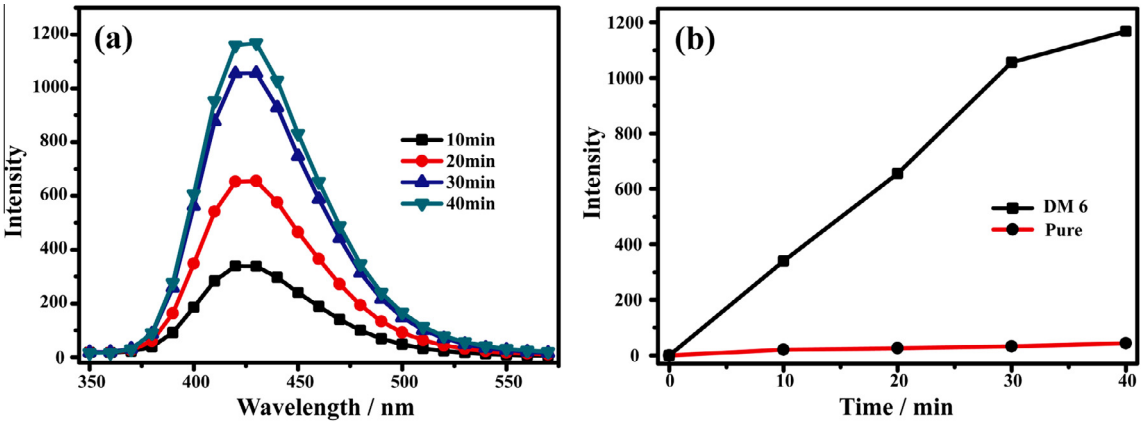

Figure 7 Fluorescence spectra of the DM 6 sample under visible light ($\lambda > 420$ nm): (a) different fluorescence spectra curves at 10, 20, 30, and 40 min; (b) the comparison of fluorescence intensity between DM 6 and pure TiO_2.

photoelectrochemical performances are influenced by not only the excitation and separation of electron–hole pairs but also the transport of charge carriers, and the final photocurrent density was determined by the synergistic function of these two factors. Therefore, the photoelectric conversion performance decreased when the Mn content was higher than 6 at.% (Fig. 6b). It is concluded that high level doping may cause too many lattice defects, which can act as recombination centers for electron and holes so that they degrade the conversion performance [39]. The competitive growth of rutile when Mn content is higher than 6% may also influence the photo sensitivity of TiO_2 [40].

The photoactivity of the manganese doped TiO_2 was estimated by detecting the generated amount of the important photocatalysis active species of ·OH radicals, terephthalic acid (TA) was used as a fluorescence probe [41]. As shown in Fig. 7a, obvious fluorescence spectra associated with 2-hydroxy TA are generated upon irradiation of the DM 6 suspended in TA solution within 350–600 nm for different irradiation times. The nearly linear relationship between fluorescence intensity and irradiation time does confirm the stability of our sample, and more importantly, the synthesized DM 6 can generate the photocatalytic ·OH radicals under >420 nm as illuminated. Only neglectable ·OH radicals can be formed for pure anatase TiO_2 under visible light irradiation.

4. Conclusion

This work induces a significant red-shift to ~600 nm in the optical absorption edges of TiO_2 so that they can be used as effective optical absorbing materials in novel photovoltaic cells with long-term sustainability or smart photo-catalysts beyond the ultraviolet range. A Mn doped TiO_2 was synthesized by the hydrothermal treatment of titanium boride and manganese chloride to get the precursor solution. TiO_2 was precipitated by adding ammonium water into the hydrothermally obtained solution. The continuous red shift was observed on the UV–Vis spectra by increasing Mn content from 0% to 10%. The remarkable improvement of about 5 times in photo current compared with that of pristine TiO_2 was obtained by Mn doping in the visible (>420 nm) light region. The spectroscopic characterization and VBXPS proved that Mn-doping induced significant band gap narrowing and contributed to the visible light driven photoelectric conversion performance.

Acknowledgments

The authors acknowledge financial support from the National Science Foundation of China (51001091, 111174256, and 91233101) and Basic Research Program, Ministry of Science and Technology of China (no. 2014CB931704).

References

[1] X.B. Chen, L. Liu, P.Y. Yu, S.S. Mao, Increasing solar absorption for photocatalysis with black hydrogenated titanium dioxide nanocrystals, Science 331 (2011) 746–750.
[2] Gang Liu, Jian Pan, Lichang Yin, Lichang Yin, John T.S. Irvine, Feng Li, Jun Tan, Philip Wormald, Hui-Ming Cheng, Heteroatom-modulated switching of photocatalytic hydrogen and oxygen evolution preferences of anatase TiO_2 microspheres, Adv. Funct. Mater. 22 (2012) 3233–3238.
[3] K. Yang, Y. Dai, B. Huang, Origin of the photoactivity in boron-doped anatase and rutile TiO_2 calculated from first principles, Phys. Rev. B 76 (2007) 195201.
[4] C. Fu, T. Li, J. Qi, J. Pan, S. Chen, C. Cheng, Theoretical study on the electronic and optical properties of Ce^{3+}-doped TiO_2 photocatalysts, Chem. Phys. Lett. 494 (2010) 117–122.
[5] D. Zhao, X. Huang, B. Tian, S. Zhou, Y. Li, Z. Du, The effect of electronegative difference on the electronic structure and visible light photocatalytic activity of N-doped anatase TiO_2 by first-principles calculations, Appl. Phys. Lett. 98 (2011) 162107.
[6] R. Asahi, T. Morikawa, T. Ohwaki, K. Aoki, Y. Taga, Visible-light photocatalysis in nitrogen-doped titanium oxides, Science 293 (2001) 269–271.
[7] A. Braun, K.K. Akurati, G. Fortunato, F.A. Reifler, A. Ritter, A.S. Harvey, et al, Nitrogen doping of TiO_2 photocatalyst forms a second eg state in the oxygen 1s NEXAFS pre-edge, J. Phys. Chem. C 114 (2010) 516–519.
[8] M. You, T.G. Kim, Y.M. Sung, Synthesis of Cu-doped TiO_2 nanorods with various aspect ratios and dopant concentrations, Cryst. Growth Des. 10 (2010) 983–987.
[9] M. Mansoob Khan, Sajid A. Ansari, M. Ikhlasul Amal, Jintae Lee, Moo Hwan Cho, Highly visible light active Ag@TiO_2 nanocomposites synthesized using an electrochemically active biofilm: a novel biogenic approach, Nanoscale 5 (2013) 4427–4435.
[10] Mohammad Mansoob Khan, Sajid Ali Ansari, Jin-Hyung Lee, M. Omaish Ansari, Jintae Lee, Moo Hwan Cho, Electrochemically active biofilm assisted synthesis of Ag@CeO_2 nanocomposites for antimicrobial activity, photocatalysis and photoelectrodes, J. Colloid Interface Sci. 431 (2014) 255–263.
[11] Mohammad Mansoob Khan, Jintae Lee, Moo Hwan Cho, Au@TiO_2 nanocomposites for the catalytic degradation of methyl orange and methylene blue: an electron relay effect, J. Ind. Eng. Chem. 20 (2014) 1584–1590.
[12] Sajid Ali Ansari, Mohammad Mansoob Khan, M. Omaish Ansari, Jintae Lee, Moo Hwan Cho, Biogenic synthesis, photocatalytic, and photoelectrochemical performance of Ag–ZnO nanocomposite, J. Phys. Chem. C 117 (2013) 27023–27030.
[13] Mohammad Mansoob Khan, Sajid Ali Ansari, M. Omaish Ansari, B.K. Min, Jintae Lee, Moo Hwan Cho, Biogenic fabrication of Au@CeO_2 nanocomposite with enhanced visible light activity, J. Phys. Chem. C 118 (2014) 9477–9484.
[14] R. Saravanan, E. Thirumal, V.K. Gupta, V. Narayanan, A. Stephen, The photocatalytic activity of ZnO prepared by simple thermal decomposition method at various temperatures, J. Mol. Liq. 177 (2013) 394–401.
[15] R. Saravanan, V.K. Gupta, T. Prakash, V. Narayanan, A. Stephen, Synthesis, thermal decomposition method, J. Mol. Liq. 178 (2013) 88–93.
[16] R. Saravanan, V.K. Gupta, V. Narayanan, A. Stephen, Visible light degradation of textile effluent using novel catalyst ZnO/g-Mn_2O_3, J. Taiwan Inst. Chem. Eng. 45 (2014) 1910–1917.
[17] R. Saravanana, H. Shankara, T. Prakasha, V. Narayananb, A. Stephen, ZnO/CdO composite nanorods for photocatalytic degradation of methylene blue under visible light, Mater. Chem. Phys. 125 (2011) 277–280.
[18] R. Saravanan, S. Karthikeyan, V.K. Gupta, G. Sekaran, V. Narayanan, A. Stephen, Enhanced photocatalytic activity of ZnO/CuO nanocomposite for the degradation of textile dye on visible light illumination, Mater. Sci. Eng. C 33 (2013) 91–98.
[19] M. Hannelore Rittmann-Frank, Chris J. Milne, Jochen Rittmann, Marco Reinhard, Thomas J. Penfold, Majed Chergui, Mapping of the photoinduced electron traps in TiO_2 by picosecond X-ray absorption spectroscopy, Angew. Chem. Int. Ed. 53 (2014) 5858–5862.
[20] G.S. Shao, Q.R. Deng, L. Wan, M.L. Guo, X.H. Xia, Y. Gao, Molecular design of TiO_2 for gigantic red shift via sublattice substitution, Nanosci. Nanotechnol. 10 (2010) 7092–7096.

[21] G. Shao, Electronic structures of manganese-doped rutile TiO_2 from first principles, J. Phys. Chem. C 112 (2008) 18677–18685.
[22] G. Shao, Red shift in manganese- and iron-doped TiO_2: a DFT + U analysis, J. Phys. Chem. C 113 (2009) 6800–6808.
[23] V.D. Binas, K. Sambania, T. Maggos, A. Katsanaki, G. Kiriakidis, Synthesis and photocatalytic activity of Mn-doped TiO_2 nanostructured powders under UV and Visible light, Appl. Catal. B 113–114 (2012) 79–86.
[24] Ruby Chauhan, Ashavani Kumar, Ram Pal Chaudhary, Structural and photocatalytic studies of Mn doped TiO_2 nanoparticles, Spectrochim. Acta Part A 98 (2012) 256–264.
[25] Lijie Wang, Jiajie Fan, Zetan Cao, Yichao Zheng, Zhiqiang Yao, Guosheng Shao, Hu Junhua, Fabrication of predominantly Mn^{4+}-doped TiO_2 nanoparticles under equilibrium conditions and their application as visible-light photocatalyts, Chem. Asian J. 9 (2014) 1904–1912.
[26] Tetsuro Kawahara, Yasuhiro Konishi, Hiroaki Tada, Noboru Tohge, Junji Nishii, Seishiro Ito, A patterned TiO_2(Anatase)/TiO_2(Rutile) bilayer-type photocatalyst: effect of the anatase/rutile junction on the photocatalytic activity, Angew. Chem. Int. Ed. 41 (2002) 15.
[27] T. Ohsaka, F. Izumi, Y. Fujiki, Raman spectrum of anatase, TiO_2, J. Raman Spectrosc. 7 (1978) 321–324.
[28] X. Chen, C. Burda, The electronic origin of the visible-light absorption properties of C-, N- and S-doped TiO_2 nanomaterials, J. Am. Chem. Soc. 130 (2008) 5018–5019.
[29] T. Ohsawa, M.A. Henderson, S.A. Chambers, Epitaxial growth and orientational dependence of surface photochemistry in crystalline TiO_2 rutile films doped with nitrogen, J. Phys. Chem. C 114 (2010) 6595–6601.
[30] Y.Q. Cao, T. He, Y. Chen, Y.A. Cao, Fabrication of rutile TiO_2–Sn/anatase TiO_2–N heterostructure and its application in visible-light photocatalysis, J. Phys. Chem. C 114 (2010) 3627–3633.
[31] M.V. Koudriachova, S.W. Leeuw, Orthorhombic distortion on Li intercalation in anatase, Phys. Rev. B 69 (2004) 054106.
[32] F.M.F. de Groot, J. Faber, J.J.M. Michiels, M.T. Czyiyk, M. Abbate, J.C. Fuggle, 1s X-ray absorption of tetravalent titanium oxides: a comparison with single-particle calculations, Phys. Rev. B 48 (1993) 2074–2080.
[33] M.M. Islam, T. Bredow, A. Gerson, Electronic properties of oxygen-deficient and aluminum-doped rutile TiO_2 from first principles, Phys. Rev. B 76 (2007) 045217.
[34] E. Cho, S. Han, H.S. Ahn, K.R. Lee, S.K. Kim, C.S. Hwang, First-principles study of point defects in rutile TiO_{2-x}, Phys. Rev. B 73 (2006) 193202.
[35] Natacha Kinadjian, Mickael Le Bechec, Thierry Pigot, Fabien Dufour, Olivier Durupthy, Ahmed Bentaleb, Eric Prouzet, Sylvie Lacombe, Rénal Backov, Photocatalytic TiO_2 macroscopic fibers obtained through integrative chemistry, Eur. J. Inorg. Chem. 32 (2012) 5350–5359.
[36] E.L. Bullock, L. Patthey, S.G. Steinemann, Clean and hydroxylated Rutile TiO_2 (110) surfaces studied by X-ray photoelectron spectroscopy, Surf. Sci. 352–354 (1996) 504–510.
[37] M. You, T.G. Kim, Y.-M. Sung, Synthesis of Cu-doped TiO_2 nanorods with various aspect ratios and dopant concentrations, Cryst. Growth Des. 10 (2010) 983–987.
[38] X.H. Xia, L. Lu, A.S. Walton, M. Ward, X.P. Han, R. Brydson, J.K. Luo, G. Shao, Origin of significant visible-light absorption properties of Mn-doped TiO_2 thin FILMS, Acta Mater. 60 (2012) 1974–1985.
[39] Junbo Guo, Zhanghua Gan, Lu Zhihong, Jing Liu, Jingjing Xi, Yang Wan, Lin Le, Hailin Liu, Jing Shi, Rui Xiong, Improvement of the photocatalytic properties of TiO_2 by (Fe + Mo) Co-doping–a possible way to retard the recombination process, J. Appl. Phys. 114 (2013) 104903.
[40] S. Won, S. Go, K. Lee, J. Lee, Resistive switching properties of $Pt/TiO_2/n+$-Si ReRAM for nonvolatile memory application, Electron. Mater. Lett. 4 (2008) 29–33.
[41] G. Liu, L.Z. Wang, C.H. Sun, X.X. Yan, X.W. Wang, Z.G. Chen, S.C. Smith, H.M. Cheng, G.Q. Lu, Band-to-band visible-light photon excitation and photoactivity induced by homogeneous nitrogen doping in layered titanates, Chem. Mater. 21 (2009) 1266–1274.